Journal of Interfaces, Thin films, and Low dimensional systems 5 (1) Summer and Autumn (2021) 421-427


# Effect of temperature changes on thermoelectric properties of the two sided-closed single-walled BNNTs (6, 3)

Scientific research paper

Ali Mohammad Yadollahi[1], Peyman Azimi Anaraki[1*], Mojtaba Yaghobi[2], Mohammad Reza Niazian[2]

[1]*Department of Physics, Takestan Branch, Islamic Azad University, Takestan, Iran*

[2]*Department of Physics, Ayatollah Amoli Branch, Islamic Azad University, Amol, Iran*

**ARTICLE INFO**

*Article history:*
Received 26 April 2022
Revised 16 June 2022
Accepted 30 June 2022
Available online 2 July 2022

*Keywords:*
Nanotube
Seebeck coefficient
Coefficient of merit
Thermal conductivity
Electrical conductivity

**ABSTRACT**

In this study, thermoelectric properties of the two sided-closed single-walled boron nitride nanotubes (TSC-SWBNNTs) are investigated. For this purpose, a nanotube with the chirality of (6, 3) is selected with no impurities. The energy is considered in the range of -5.5 to 5.5 electron volts as the investigations are performed at temperatures 300, 500, 700 and 900K. The results show that increasing temperature results in significant reduction in the length of the bandgap. Besides, the peaks of the conduction diagram become smaller and their number decreases, indicating the return of more electrons and holes around the LUMO and HOMO bands, respectively, which leads to reduction of the bandgap and increase in the conduction. Moreover, the seebeck coefficient (thermal power) increases to about 370 μV/K by increasing temperature to 900K. As the temperature increases, the coefficient of merit (ZT) increases to about 0.95, and it is expected to experience more increase with further increase in temperature. Thermal conductivity increases slightly with increasing temperature. However, the values of thermal conductivity are at the nanoscale. Therefore, in general, it can be concluded that the (TSC-SWBNNT) (6, 3) can be selected as a suitable thermoelectric material.

## 1 Introduction

When a conductor or semiconductor material is subjected to a temperature difference and electrical conductivity is established in it, it is discussed in the thermoelectric field [1]. Applying a temperature difference between two ends of a material, results in increasing the energy of the charge carriers on the hot side of the material. Hence these carriers are excited and tend to penetrate from the hot zone to the cold zone. With the accumulation of carriers in the cold part of the material, the charge neutralization is lost and an internal electric field is formed which prevents further migration of the carriers. Eventually an equilibrium is reached and an electric voltage difference is created according to the temperature gradient [2].

ZT is a thermoelectric characteristic that depends on both electrical and thermal conductivity. High ZT requires high seebeck coefficient, high electrical conductivity and low thermal conductivity [3]. Furthermore, increasing the temperature increases the ZT. Phonon conduction is different from electron conduction. The mean free path of electrons is only from a few angstroms to a few nanometers. While, depending on the crystal structure and microstructure of the material, the mean free path of phonons is from a

*Corresponding author.
Email address: Peyphysics2004@Yahoo.co.uk
DOI: 10.22051/jitl.202.40200.1072

few nanometers to several hundred micrometers. As a result, scattering sites with a length scale greater than a few nanometers cannot have a considerable effect on electrons, while they can effectively scatter phonons. This phenomenon is known as an effective approach to reduce the thermal conductivity of the lattice while having a minor effect on the electrical conductivity. This strategy is called nanostructured thermoelectrics or small dimension [4-7].

By reducing the size of the system to nanometer dimensions, it is possible that significant changes occur in the electron density of states, leading to changes in the seebeck coefficient, electrical conductivity, and thermal conductivity. For the sufficiently small lengths, and the effect of quantum constraint see Ref [8].

Nanotubes are one-dimensional nanostructures whose electronic and thermoelectric transport have been considered extensively. Carbon nanotubes (CNTs) have unique mechanical, electrical, and thermal properties which leads to their applications in different fields such as construction of transistors and heat transport [9]. Phonons play a major role in the thermal conductivity of nanotubes and are 100 times more effective in the heat capacity of CNTs than the electrons [10]. The mean free path length of phonons in nanotubes is estimated in the order of micrometers. However, this length decreases due to phonon scattering resulting from phonon-phonon, phonon-boundary, and phonon-defect interactions [11]. Boron nitride nanotubes (BNNTs), with high biocompatibility properties, have better electrical and thermal properties compared to CNTs. They were first predicted in 1994 [12-17] and synthesized experimentally a year later [18].

Since Boron nitride nanotubes are composed of nitrogen and boron atoms, due to the electronegativity difference between these elements, the B-N bonds would be partially ionic. Caused by this electronegativity difference, a band of 5-6 electron volts is created for Boron nitride nanotubes, which is not dependent on the chirality and its diameter [12-14]. CNTs are resistant to oxidation up to 500 °C, while this temperature is 1000 °C for boron nitride nanotubes [19-20]. Since increasing the temperature increases the ZT, so a higher ZT can be achieved by further increasing the temperature to 1000 °C for boron nitride nanotubes. In this study, thermoelectric properties of the two sided-closed single-walled boron nitride nanotube (6, 3) ((TSC-SWBNNT) (6, 3)) between two electrodes made by (5, 5) CNTs has been examined at different temperatures (See Figure (1)).

## 2 Method

In this research, the ATK simulation software is used. According to Figure 2, the considered TSC-SWBNNT consists of 60 $N$ and 60 $B$ atoms. The diameter and length of this nanotube is about 6.1 and 15.6 Å, respectively.

In this study, Slater-Koster [21] and ForceField [22] methods along with tight-binding approximation and non-equilibrium Green function (NEGF) are used. The two sides of the nanotube are closed using pentagons and hexagons made of boron and nitrogen atoms. The (TSC-SWBNNT) (6, 3) is connected to the electrodes using a hexagon made of boron and nitrogen atoms. The plate passing through this hexagon is located parallel to the cross section of the electrodes at both sides of the nanotube.

The axis of the (TSC-SWBNNT) (6, 3) is considered parallel to the z-axis. During the simulation, the mesh cut off is equal to 150 Ridberg [23-24]. Besides, brillouin area zone K-point is considered as $1 \times 1 \times 100$ [22-23].

To optimize the device, a force tolerance of 0.01 eV/Å with a maximum of 500 steps is used. To obtain thermoelectric properties, energy range is considered in the range of -5.5 to 5.5 eV while the bias voltage is selected in the range of 0 to 5 volts. CNTs with the chirality of (5, 5) and $1 \times 1 \times 4$ repetitions are employed in the electrodes.

In this study, thermoelectric properties including electrical conductivity, thermal conductivity, Seebeck coefficient, and ZT of pure (TSC-SWBNNT) (6, 3) at the temperatures of 300, 500, 700, and 900K are investigated. The transmission function T (E, V) according to the NEGF relationship with energy E and bias voltage V is obtained by the following relation [23-25]:

$$T(E,V) = Tr[\Gamma_L(V)G^R(E,V)\Gamma_R(V)G^A(E,V)], \quad (1)$$

where $G^R$ and $G^A$ are the retarded and advanced Green functions of the central scattering region, respectively.

$\Gamma_{LR} = i[\sum_{L(R)}^{R}(E) - \sum_{L(R)}^{A}(E)]$ is broadening function, $\sum_{L(R)}^{R}(E)$ and $\sum_{L(R)}^{A}(E)$ are the self-energies of the central scattering region that include all the effects of the electrodes [25-26]. System current is expressed by the Landauer-Butikker formula [26-28]:

$$I(V) = \frac{2e}{h}\int [f(E-\mu_L) - f(E-\mu_R)]T(E,V)dE, \quad (2)$$

where h is Planck's constant, e is electron charge, $f(E-\mu_{L(R)})$ is function of the Fermi distribution of electrons in the left (right) electrode, and $\mu_{L(R)}$ is the electrochemical potential of the left (right) electrode [26-28].

In the linear response region, thermoelectric coefficients arising from applying a voltage difference (dV) or temperature difference (dT) between the two electrodes are obtained using the following equations. Equation (3) is used to compute the electrical conductivity (Ge) [29-30]:

$$G_e = \left.\frac{dI}{dV}\right|_{dT=0}. \quad (3)$$

The Peltier coefficient which is used in cooling machines is obtained as [30-31]:

$$\Pi = \left.\frac{I_Q}{I}\right|_{dT=0}. \quad (4)$$

The Seebeck coefficient (thermal power) is equal to [29-30]:

$$S = -\left.\frac{dV}{dT}\right|_{I=0} = \frac{\Pi}{V}. \quad (5)$$

The thermal conductivity, which is the sum of the electron thermal conductivity and the phonon thermal conductivity, is obtained by the following relation [29-30]:

$$\kappa = \kappa_e + \kappa_{ph} = \left.\frac{dI_Q}{dT}\right|_{I=0}. \quad (6)$$

The heat current is obtained from the following equation [29-30]:

$$I_Q = dQ/dT, \quad (7)$$

The dimensionless thermoelectric coefficient (ZT) is obtained as [29-30]:

$$ZT = \frac{G_e S^2 T}{k}, \quad (8)$$

In this equation $G_e$, $S$, $T$, and $k$ represent the electrical conductivity, Seebeck coefficient, Kelvin temperature, and thermal conductivity, respectively.

The above relations show how applying a temperature difference leads to a voltage difference in a thermoelectric material. These coefficients in the linear response area are calculated by the thermoelectric coefficients plugged in the ATK software.

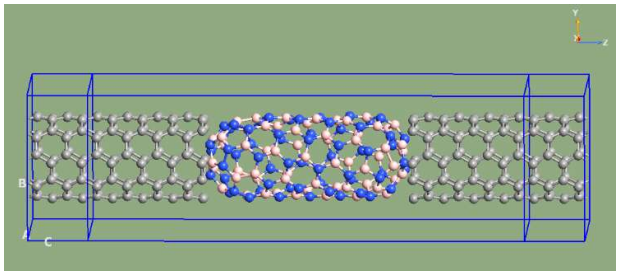

Figure 1. Device made with pure (TSC-SWBNNT) (6, 3) and two (5, 5) carbon nanotube electrodes on both sides.

## 3 Results and discussion

Electrical conduction diagram of the (TSC-SWBNNT) (6, 3) are depicted in Figure 3 at different temperatures including 200, 300, 500, 700, and 900 K. As the temperature increases, the movement of electrons and ions (phonons) increases and the number of charge carrier densities increases. This increases the probability of electrons and phonons colliding which reduces their mean free path of electrons and phonons. Phonon conduction is different from electron conduction. The mean free path of electrons is only from a few angstroms to a few nanometers. While, depending on the crystal structure and microstructure of the material, the mean free path of phonons is from a few nanometers to several hundred micrometers. As a result, scattering sites with a length scale greater than a few nanometers cannot have considerable effect on electrons, while they can effectively scatter phonons. This phenomenon is known as an effective approach to reduce the thermal conductivity of the lattice while having a minor effect on the electrical conductivity. According to Figure 3, the bandgap decreases significantly by increasing the temperature. At 200 K,

the number of peaks observed in the graph is larger than other temperatures. Hence, it can be concluded that increasing temperature results in decreasing the number of peaks. This indicates that the motion of electrons and holes increases and their localization decreases at larger temperatures.

As the temperature rises from 200 to 900 K, the height of the main peaks decreases. This means that greater number of electrons and holes are gathered in the LUMO (highest capacity) and HOMO (lower capacity) edges respectively for further conduction while the peak heights are reduced at energies lower than the HOMO band and higher than the LUMO band. At about 0.25 eV, a small conduction peak of $1 \times 10^{-6}$ can be seen, which slightly affects the bandgap.

Figure 4 shows the Seebeck coefficient (thermal power) in terms of energy at the temperatures of 200, 300, 500, 700, and 900 K. It is observed that by increasing temperature, the height of the peaks increases while the number of peaks decreases. This shows that although the value of Seebeck coefficient increases at larger temperatures, the localization of electrons and holes decreases. The maximum value of Seebeck coefficient has increased from about 260 μV/K in the range of 0.3 eV to about 370 μV/K in the range of 0.5 eV. Maximum of the Seebeck coefficient occurs at the temperature of 500K, which slightly decreases by increasing the temperature to 900K.

Thermal conductivity of (6,3) TSC-SWBNNT at temperatures of 200, 300, 500, 700, and 900 K is represented in Figure 5 in terms of energy at temperatures of 300, 500, 700, and 900 K. It is seen that by increasing the temperature, the height of heat conduction curves increases and the thermal conductivity possesses larger values. However, the values of thermal conductivity in Figure 5 are at the nanoscale, which are small compared to values of the Seebeck coefficient (see Figure 4) and the electrical conductivity (see Figure 3).

Figure 6 represents the merit coefficient (ZT) of (TSC-SWBNNT) (6, 3) at temperatures of 300, 500, 700, and 900 K. As it can be seen in this figure, the height of the peaks increases by increasing temperature, which indicates an increase in ZT. Instead, the number of peaks decreases at larger temperatures, which means that by increasing the mobility of electrons and holes at larger temperatures, their localization decreases. The maximum of ZT increases from about 0.4 at 200 K to about 0.95 at 900 K. Furthermore, around 0.25 eV, two small values of ZT (in order of 0.01) are observed. In the energy of -2.25 eV, the peak is about 0.4 at the temperature of 900K. This peak decreases by decreasing temperature. With further increasing temperature, it can be expected that the value of the merit coefficient increases. This indicates that (TSC-SWBNNT) (6, 3) can be a suitable thermoelectric material.

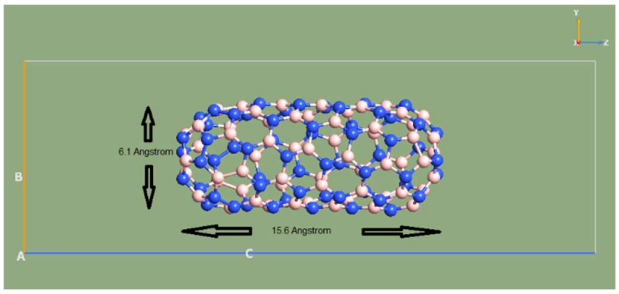


Figure 2. Considered (TSC-SWBNNT) (6, 3).

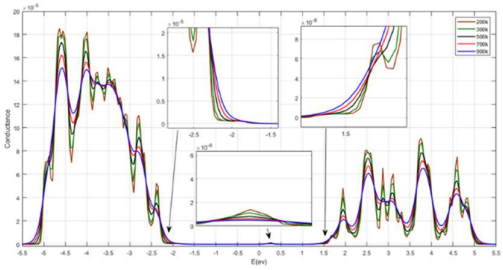

Figure 3. Conductance diagrams of (TSC-SWBNNT) (6, 3) at temperatures of 200, 300, 500, 700, and 900K.

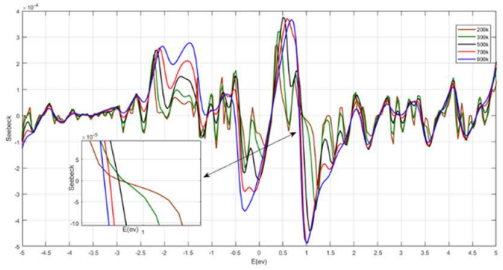

Figure 4. Seebeck coefficient of (TSC-SWBNNT) (6, 3) at temperatures of 200, 300, 500, 700, and 900K.

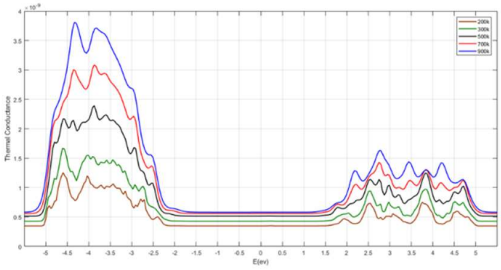

Figure 5. Thermal conductivity of (TSC-SWBNNT) (6, 3) at temperatures of 200, 300, 500, 700, and 900K.

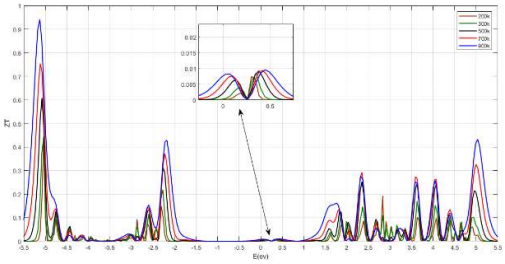

Figure 6. Merit coefficient (ZT) of (TSC-SWBNNT) (6, 3) at temperatures of 200, 300, 500, 700, and 900K.

## 4 Conclusions

In this study, the thermoelectric properties of pure (TSC-SWBNNT) (6, 3) were investigated. For this purpose, the energy range was considered as -5.5 to 5.5 eV. Besides, the simulations were performed at different temperatures including 300, 500, 700, and 900K. The results showed that by increasing temperature, the bandgap decreases significantly. In addition, the coefficient of Seebeck (thermal power) and ZT increased significantly by increasing the temperature.

The results of this research can be summarized as follows:

1- By increasing temperature, the bandgap decreases significantly on both sides, which indicates increase in the conductivity of the material. In this study, a diode mode is used, ie the nanotube is located between the two electrodes of the drain and the source. If a gate voltage is also applied to the device (Transistor mode), this will further reduce the bandgap and other changes [31].
2- By increasing temperature and decreasing the bandgap, more electrons and holes move towards the band of LUMO and HOMO, respectively. Hence, the height of the conduction peaks and their number decrease. Besides, the localization of electrons and holes also reduce.
3- By increasing temperature, the Seebeck coefficient (thermal power) increases from about 260 µV/K to about 370 µV/K.
4- By increasing temperature, in the presence of phonons thermal conductivity also slightly increases. However, its increase is as small as the nano ($10^{-9}$) range.
5- The value of coefficient of merit (ZT) increases by increasing the temperature to about 0.95. It is expected that by more increasing temperature, this coefficient increases more and goes above 1.
6- According to the results, it can be concluded that (TSC-SWBNNT) (6, 3) can be considered as a suitable thermoelectric material.
7- The investigated nanotube is in pure state. It is expected that the injection of various impurities can significantly increase the value of the coefficient of merit (ZT).

## References

[1] T. M. Tritt, "Thermoelectric phenomena, materials, and applications." Annual Review of Materials Research, **41** (2011) 433.

[2] S. LeBlanc, "Thermoelectric generators: Linking material properties and systems engineering for waste heat recovery applications". Sustainable Materials and Technologies, **1** (2014) 26.

[3] G. J. Snyder and E. S. Toberer. "Complex thermoelectric materials". Nature Materials, **7** (2008) 105.

[4] A. Minnich et al. "Bulk nanostructured thermoelectric materials: current research and future prospects." Energy & Environmental Science, **2** (2009) 466.

[5] M. Zebarjadi et al., "Perspectives on thermoelectrics: from fundamentals to device applications." Energy & Environmental Science, **5** (2012) 5147.

[6] M. S. Dresselhaus et al., "New Directions for Low-Dimensional Thermoelectric Materials." Advanced Materials, **19** (2007) 1043.

[7] Y. Lan et al., "Enhancement of Thermoelectric Figure-of-Merit by a Bulk Nanostructuring Approach." Advanced Functional Materials, **20** (2010) 357.

[8] M. S. Dresselhaus et al., "New Directions for Low-Dimensional Thermoelectric Materials," Advanced Materials, **19** (2007) 1043.

[9] A. M. Marconnet et al., "Thermal conduction phenomena in carbon nanotubes and related nanostructured materials." Reviews of Modern Physics, **85** (2013) 1295.

[10] L. X. Benedict et al., "Heat capacity of carbon nanotubes." Solid State Communications, **100** (1996) 177.

[11] Z. Wang et al. "Length-dependent thermal conductivity of single-wall carbon nanotubes: prediction and measurements." Nanotechnology, **18** (2007) 475714.

[12] Blase X. Blase et al. "Stability and band gap constancy of boron nitride nanotubes." Europhysics Letters, **28** (1994) 335.

[13] A. Rubio et al., "Theory of graphitic boron nitride nanotubes." Physical Review B, **49** (1994) 5081.

[14] C. H. Lee et al., "Patterned growth of boron nitride nanotubes by catalytic chemical vapor deposition." Chemistry of Materials, **22** (2010) 1782.

[15] M. L. Cohen and A. Zettl. "The physics of boron nitride nanotubes." Physics Today, **63** (2010) 34.

[16] A. L. Tiano et al. "Boron nitride nanotube: synthesis and applications in Nanosensors, Biosensors, and Info-Tech Sensors and Systems." International Society for Optics and Photonics, **9060** (2014) 906006.

[17] C. Lee et al. "Boron nitride nanotubes: recent advances in their synthesis, functionalization and applications." Molecules, **21** (2016) 922.

[18] N. G. Chopra et al., "Boron nitride nanotubes." Science, **269** (1995) 966.

[19] Mohammad Yaghobi et al., "Magnetic and structural properties of BNC nanotubes." Molecular Physics, 117 (2019) 260.

[20] J. X. Zhao and B.Q. Dai. "DFT studies of electro-conductivity of carbon-doped boron nitride nanotube." Materials Chemistry and Physics, **88** (2004) 244.

[21] D. A. Papaconstantopoulos and M. J. Mehl. "The Slater–Koster tight-binding method: a computationally efficient and accurate approach." Journal of Physics: Condensed Matter, **15** (2003) 413.

[22] Julian Schneider et al., "ATK-ForceField: a new generation molecular dynamics software package." Modelling and Simulation in Materials Science and Engineering, 25 (2017) 085007.

[23] P. Zhao et al. "Rectifying behavior in nitrogen-doped zigzag single-walled carbon nanotube junctions." Solid State Communications, **152** (2012) 2040.

[24] Mei Wang et al. "Spin transport properties in Fe-doped graphene/hexagonal boron-nitride nanoribbons heterostructures." Physics Letters A, **383** (2019) 2217.

[25] S. Datta. Electronic Transport in Mesoscopic Systems. Cambridge University Press. New York 1995.

[26] P. Chaudhuri et al. "Density functional study of glycine adsorption on single-walled BN nanotubes." Applied Surface Science, **536** (2020) 147686.

[27] J. X. Zhao et al. "A Theoretical Study on the Conductivity of Carbon Doped BNNT". Chemical Society, **52** (2005) 395.

[28] Chenkang Rui et al. "Transport properties of B/P doped grapheme nanoribbon field-effect transistor." Materials Science in Semiconductor Processing, **130** (2021) 105826.

[29] N. Hilaal Alama and Seeram Ramakrishnab. "A review on the enhancement of figure of merit from bulk to nano-thermoelectric materials." Nano Energy, **2** (2013) 190.

[30] T. M. Tritt. Encyclopedia of Materials: Science and Technology, Thermoelectric Materials: Principles, Structure, Properties, and Applications. Elsevier Science Ltd (2002).

[31] A. M. Yadollahi, P. Azimi Anaraki, M. Yaghobi, Thermoelectric properties of two sided-closed single-walled boron nitride nanotubes (6, 3). Indian Journal of Physics, (2022).